Biophys. Struct. Mech. 7, 1–16 (1980)

Biophysics of Structure and Mechanism

Nonequilibrium Ion Transport Through Pores*

The Influence of Barrier Structures on Current Fluctuations, Transient Phenomena and Admittance

E. Frehland and K. H. Faulhaber

Universität Konstanz, Fakultät für Physik,
Postfach 5560, D-7750 Konstanz, Federal Republic of Germany

Abstract. In this paper is presented an investigation of the influence of the internal structure of pores in membranes on a) the time dependent macroscopic relaxation current after a voltage jump, b) the macroscopic frequency dependent admittance and c) the microscopic current fluctuations around stationary (nonequilibrium) states. All these quantities are determined by the time dependent transport equations, which are calculated with the use of the eigenvectors and eigenvalues of the matrix of coefficients, occurring in the transport equations. Numerical calculations for channels with up to 31 barriers are presented. The treatment of the fluctuations is done with the use of a general approach to nonequilibrium transport noise recently developed by one of the authors. It is shown that the influence of the internal barrier structure as, e.g., the height of central or decentral barriers in the pores is of great complexity. Nevertheless we hope that the calculations lead to a better understanding especially of the microscopic nonequilibrium transport fluctuations in complex systems.

Key words: Ion transport through pores – Nonequilibrium steady state – Jump diffusion – Barrier structure

Introduction

The mechanisms of ion transport through biological membranes are not yet completely clarified. But it seems likely that in many cases the transport of ions is made possible by hydrophobic porous structures within the membranes, which are built up by proteins. Such a pore or channel may be considered as a sequence of activation barriers, separated by energy minima (binding sites) [1, 2]. The internal structure of membrane channels, such as the number of binding sites and the height of internal barriers has been subject of considerable interest and speculation [3–5].

* This work has been supported by the Deutsche Forschungsgemeinschaft

0340-1057/80/0007/0001/$ 03.20

In this paper we present a systematic investigation of the influence of the barrier structure in membrane channels on the time-dependent macroscopic current, the macroscopic admittance and on the microscopic current fluctuation mainly under nonequilibrium conditions. The channels or pores are assumed to be permanently open. Interactions between the ions are neglected, so that oscillatory transport phenomena [6] cannot occur. The time dependent solutions of the transport equations, by which the macroscopic current as well as the admittance and the microscopic fluctuations are determined, are calculated with the use of the eigenvectors and eigenvalues of the matrices of coefficients, occurring in the transport equations. The eigenvectors and eigenvalues are determined numerically by evaluation of the symmetrized matrices. The developed numerical programs make possible the treatment of arbitrary barrier structures. Examples for channels with up to 31 barriers are presented. For each considered barrier structure the time dependent current relaxation to a new stationary state after a sudden voltage jump and the frequency dependent admittance as well as the spectral density and autocorrelation function of current fluctuations around this state are calculated. The treatment of fluctuations is done with the use of a general approach to current fluctuations in discrete transport systems, recently developed by one of the authors [7–9].

This paper continues our systematic investigations of ion transport through porous structures. Chapter 2 contains a recapitulation of the theoretical background as far as necessary. In chapter 3 are presented the numerical model calculations.

The results demonstrate a great complexity of the behaviour of the transport system as a function of the internal barrier structure of the pores and may serve as a warning against specific and detailed conclusions from experimental results concerning the internal fine structure of pores.

In all calculations we have chosen values of the rate constants around the order one in arbitrary units. Obviously only the relative magnitude of the rate constants has been important for the analysis. In ionic channels through biological membranes the typical times are still too fast for the presently available experimental methods in the time- as well as in the frequency domain. But we hope that in the near future the improvement of the experimental methods will make possible an experimental analysis.

2. The Transport Model

a) General Equations

The transport system consists of a membrane separating two ionic solutions and containing a great number of identical pores (channels). It is assumed that only one ion species may penetrate the channels. The concentrations of this ion species at the pore mouths in both solutions are assumed to be held constant.

Throughout this paper interactions between the pores and between the ions are neglected. The effects of interactions between the ions in a single-file

diffusion model, e.g., the occurrence of damped oscillations, have recently been discussed [6]. In this paper we are mainly interested in the effects of a specific barrier structure on the ion transport.

The pores are considered to be a sequence of (n+1) activation barriers separated by n energy minima (binding sites) [2, 3]. The rate constants for jumps from the i-th binding site to the right or to the left are denoted by k_i', k_i'', respectively. Jumps are possible only between neighbouring sites. The state of the transport system is described by a set of variables N_i, $i = 1, 2, \ldots n$, characterizing the occupation numbers of ions at the i-th binding site. The time-dependence of the expectation values $\langle N_i(t)\rangle$ is given by the linear phenomenological equations [2, 7]

$$\frac{d\langle N_i\rangle}{dt} = \sum_{j=1}^{n} M_{ij}\langle n_j\rangle + Y_i \tag{2.1}$$

with the stationary solutions N_i^s of the equations

$$\sum_{j=1}^{n} M_{ij}N_j^s + Y_i = 0\,. \tag{2.2}$$

The matrix $\mathbf{M}$ with the elements M_{ij} is given by the rate constants:

$$M_{ii} = -(k_i' + k_i'')\,,$$

$$M_{i,\,i+1} = k_{i+1}'',\; M_{i+1,\,i} = k_i'\,,$$

$$M_{ik} = 0 \;\text{ otherwise.} \tag{2.3}$$

The vector $\mathbf{Y}$ (inhomogeneity) with components Y_i is determined by the contact of the pores with the left- and right-hand solutions (reservoirs)

$$Y_1 = k_0' N_0,\; Y_n = k_{n+1}'' N_{n+1},\; Y_i = 0 \;\text{ otherwise.} \tag{2.4}$$

N_0, N_{n+1} are the concentrations at the pore mouths and assumed to be constant, and k_0', k_{n+1}'' are the rate constants for jumps into the pores from the left, right solutions respectively. According to Onsager's regression hypothesis the Eq. (2.1) describe as well the time dependent relaxation of $N_i(t)$ after a macroscopic disturbance.

The deviations

$$\alpha_i = N_i - N_i^s \tag{2.5}$$

from the stationary states satisfy the homogeneous equations

$$\frac{d\langle\alpha_i\rangle}{dt} = \sum_{j=1}^{n} M_{ij}\langle\alpha_j\rangle\,. \tag{2.6}$$

The fundamental solutions $\Omega_{ik}(t)$ of (2.6) and (2.1) are solutions $\langle \alpha_i(t) \rangle$ which distinguish the k-th binding site at $t = 0$.

$$\Omega_{ik}(t) = \langle \alpha_i(t) \rangle_{\langle \alpha_i(0) = \delta_{ik} \rangle} . \tag{2.7}$$

The fundamental matrix $\Omega(t)$ with coefficients $\Omega_{ik}(t)$ represents the general solution of (2.5) and (2.1) for arbitrary initial conditions

$$\langle \alpha_i(t) \rangle = \sum_{j=1}^{n} \Omega_{ij} \langle \alpha_j(0) \rangle ,$$

$$\langle N_i(t) \rangle = \langle \alpha_i(t) \rangle + N_i^s . \tag{2.8}$$

From the special structure (2.3) of the relaxation matrix $\mathbf{M}$ it follows immediately, that $\mathbf{M}$ may be symmetrized and the eigenvalues are real and negative.

Hence $\mathbf{M}$ can be diagonalized to $\hat{\mathbf{M}}$ by an appropriate matrix $\mathbf{V}$ with components V_{ik}. The fundamental solutions are then given by

$$\Omega_{ik}(t) = \sum_{j=1}^{n} V_{ij}^{-1} \, e^{-\lambda_j t} \, V_{jk} . \tag{2.9}$$

$\mathbf{V}^{-1}$ is the inverse matrix of $\mathbf{V}$ and $-\lambda_j$, $j = 1, 2, \ldots, n$ are the negative eigenvalues of $\mathbf{M}$.

The expectation value of the total flux $\langle \phi_i \rangle$ over the i-th barrier is

$$\langle \phi_i \rangle = \langle \phi_i' \rangle - \langle \phi_i'' \rangle \tag{2.10}$$

with the unidirectional fluxes

$$\langle \phi_i' \rangle = k_{i-1}' \langle N_{i-1} \rangle , \quad \langle \phi_i'' \rangle = k_i'' \langle N_i \rangle . \tag{2.11}$$

Then the measured electric current J is given by a linear combination of the ϕ_i

$$J = \sum_{j=1}^{n+1} \gamma_i \phi_i , \tag{2.12}$$

where the constants γ_i take into account the contribution to the electric current from the jumps over the i-th barrier. They depend on geometric properties (e.g., distances between the binding sites) and dielectric properties of the membrane-pore system.

b) Relaxation Current After a Voltage Jump

For the voltage dependence of the rate constants k_i', k_i'' we use the ansatz [10]

$$k_i' = \overline{k_i'}\, e^{-\alpha_{i+1}\frac{u}{2}}, \quad k_i'' = \overline{k_i''}\, e^{-\alpha_i \frac{u}{2}}$$

$$u = \frac{ze_0 V}{kT} \tag{2.13}$$

(k: Boltzmann constant, T: absolute temperature, ze_0: ionic charge).

The dimensionless numbers α_i denote the fractions $\Delta V_{i/V}$ of the total applied voltage between the binding sites $i-1$ and i. In [9] we have given arguments based on an energy balance that α_i and the current contributions γ_i by ionic jumps between the binding sites $i-1$ and i are equal apart from the factor ze_0

$$\alpha_i z e_0 = \gamma_i \,. \tag{2.14}$$

Now consider the system to be in a stationary state with an applied voltage V_0 and stationary current $J^s(V_0)$. The stationary occupation numbers $N_i^s(V_0)$ are determined by (2.2) with M_{ij} and Y_i according to (2.3) given by (2.13). If at time $t = 0$ a sudden change in voltage (voltage jump) to V is applied, the transition of the system to the new stationary state $N_i^s(V)$ can be measured as a relaxation current J. This relaxation current can be calculated from (2.11) and (2.12) using the representation (2.8) by the fundamental solutions:

$$J = J^s(V) + \sum_{i,k=1}^{n} \Omega_{ik}(V, t)\,[N_k^s(V_0) - N_k^s(V)]\,(\gamma_{i+1}\, k_i' - \gamma_i k_i'') \,, \tag{2.15}$$

In (2.15) the fundamental solutions $\Omega_{ik}(V, t)$ can be calculated from (2.9).

c) Autocorrelation Function and Spectral Density of Current Fluctuations

The derivation of an expression for the autocorrelation function $C_{\Delta J}(t)$ of the fluctuating part

$$\Delta J = J - J^s \,. \tag{2.16}$$

(J^s = stationary current) has been done through a determination of the correlations between individual fluxes [7] and then summing up over these correlations:

$$C_{\Delta J}(t) = \sum_{j=1}^{n+1} \gamma_i^2 (\phi_i'^s + \phi_i''^s)\delta(t) + \sum_{i,k} \Omega_{ki}(t)\phi_i'^s(\gamma_i\,\gamma_{k+1}\,k_k' - \gamma_i\,\gamma_k\,k_k'')$$

$$+ \phi_{i+1}''(\gamma_{i+1}\,\gamma_k\,k_k'' - \gamma_{i+1}\,\gamma_{k+1}\,k_k') \,, \tag{2.17}$$

$\phi_i^{'s}$, $\phi_i^{''s}$ are the stationary unidirectional fluxes over the i-th barrier [c.f. (2.11)]. Introducing the time constants

$$\tau_j = \frac{1}{\lambda_j} \tag{2.18}$$

and expression (2.10) for the fundamental solutions one gets from (2.17) according to the Wiener-Khintchine relations

$$G_{\Delta J}(\omega) = 4\, Re \int_0^\infty C_{\Delta J}(t) e^{i\omega t} dt \tag{2.19}$$

the spectral density of current fluctuations

$$\begin{aligned} G_{\Delta J}(\omega) = {} & 2 \sum_{i=1}^{n+1} \gamma_i^2 \langle \phi_i^{'s} + \phi_i^{''s} \rangle + 4 \sum_{l=1}^{n} \tau_l (1 + \omega^2 \tau_l^2)^{-1} \sum_{i,k=1}^{n} V_{kl}^{-1} V_{li} \\ & \times [\phi_i^{'s} (\gamma_i \gamma_{k+1} k_k^{'} - \gamma_i \gamma_k k_k^{''}) \\ & + \phi_{i+1}^{''s} (\gamma_{i+1} \gamma_k k_k^{''} - \gamma_{i+1} \gamma_{k+1} k_k^{'})] . \end{aligned} \tag{2.20}$$

The spectrum consists of a shot noise (white noise) term and a sum of Lorentzian $(1/\omega^2)$-noise terms.

d) Admittance

At equilibrium the power spectrum $G_{\Delta J}(\omega)$ of the electric current fluctuations is according to the Nyquist theorem or fluctuation dissipation theorem given by the real part $Re\ Y(\omega)$ of the frequency dependent complex admittance $Y(\omega)$

$$G_{\Delta J}(\omega) = 4\, kT\, Re\, Y(\omega) \tag{2.21}$$

(k = Boltzmann constant, T = absolute temperature).

At nonequilibrium the admittance is defined as follows: assuming that additionally to the constant voltage V^s a small (complex) voltage

$$\varepsilon(t) = \varepsilon_0 e^{i\omega t} \tag{2.22}$$

is applied, the corresponding linear response of current $J(t)$ is

$$J(t) = J^s + j(\omega, t) \tag{2.23}$$

with the stationary current

$$J^s(V^s) = \lambda^s(V^s) \cdot V^s \tag{2.24}$$

(λ^s: macroscopic conductance)
and the frequency and time-dependent response

$$j(V^s, \omega, t) = \varepsilon_0 Y(\omega, V^s) e^{i\omega t} . \tag{2.25}$$

The differential complex *admittance* $Y(\omega, V^s)$ of the system is defined by (2.25).

In [9] we have derived a general expression for the admittance. For comparison of the fluctuation spectra with the Nyquist theorem we are especially interested in the real part of the admittance, which in the case of the discussed pore transport model is

$$\begin{aligned} 4\,kT\,Re\,Y(\omega) = {} & 2\sum_{i=1}^{n+1} \gamma_i^2 (\phi_i'^s + \phi_i''^s) \\ & + 2\sum_{l=1}^{n} \tau_l (1 + \omega^2 \tau_l^2)^{-1} \sum_{i,k=1}^{n} V_{kl}^{-1} V_{li} \\ & \times [(\phi_i'^s + \phi_i''^s)(\gamma_i \gamma_{k+1} k_k' - \gamma_i \gamma_k k_k'') \\ & + (\phi_i'^s + \phi_{i+1}''^s)(\gamma_{i+1} \gamma_k k_k'' - \gamma_{i+1} \gamma_{k+1} k_k')] . \end{aligned} \tag{2.26}$$

Comparison of (2.26) with (2.20) shows that the high frequency limits are equal, while otherwise $G_{\Delta J}(\omega)$ and $4\,kT\,Re\,Y(\omega)$ agree only at equilibrium, where according to the principle of detailed balance holds

$$\frac{1}{2}(\phi_i'^s + \phi_i''^s) = \phi_i'^s = \phi_i''^s . \tag{2.27}$$

3. Numerical Calculations

The matrix **M** of coefficients in the transport equations (2.1) may be symmetrized. Then the eigenvalues and transformation matrix **V** and its inverse $\mathbf{V}^{-1}$, by which **M** is diagonalized, can be computed by standard mathematical procedures.

We have done a number of calculations for different barrier structures of the pores using programmes available at the "Rechenzentrum" of the University of Konstanz. From the eigenvalues and transformation matrix the relaxation current after a voltage jump, the spectral density and autocorrelation function of current fluctuations and the admittance function can be calculated with (2.15), (2.17), (2.20), (2.26) respectively. All numerical calculations and plots, have been performed at the TR 440 of the University of Konstanz.

a) Equilibrium Fluctuations

We first present model calculations in order to investigate the influence of the barrier structure of the pores on the spectral density and autocorrelation function of current fluctuations at equilibrium ($J^s = 0$). In this case 4 kT times the real part of the admittance is equal to the spectral density according to the fluctuation dissipation theorem (2.21). The results are shown in the following two figures. On the right-hand side of each figure the treated potential profiles are drawn qualitatively in a suitable logarithmic presentation. The (time symmetric) autocorrelation function $C_{\Delta J}(t)$ is calculated for times $t > 0$. The delta-shaped shot noise term at $t = 0$ has been omitted. But according to (2.20), the magnitude of shot noise can be seen from the high frequency white limit of the spectral density.

The results shown in the two figures demonstrate the influence of the height of an internal barrier and of barriers at the pore mouths on the fluctuations. We

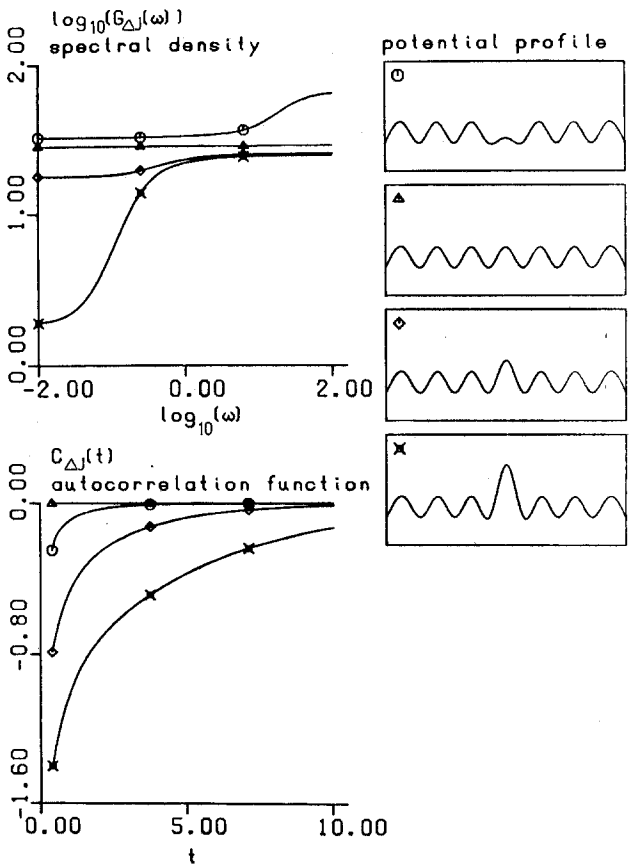

Fig. 1. Equilibrium current fluctuations in pores: variation of the height of the central barrier. $n = 6$, $N_0 = N_{n+1} = 1$, $k_i' = k_i'' = 1$ for $i = 0, 1, \ldots, n+1$ with the exceptions $k_3' = k_4'' = \circ$ 10; $\triangle$ 1; $\Diamond$ 0.2; $\bowtie$ 0.01. All γ_i are chosen to be equal

have chosen model pores with six internal binding sites ($n = 6$). The chosen values of the rate constants are given in the legends. The constant concentrations N_0, N_{n+1} at the pore mouths are set equal to one. For simplicity all γ_i, i.e., the contributions by individual jumps to the measured current, are set equal. $G_{\Delta J}(\omega)$ and $C_{\Delta J}(t)$ are calculated in arbitrary units, which on the other hand are equal in all figures except Fig. 7. In all figures the scale is chosen automatically by the graphic program.

The results confirm general properties of transport noise at equilibrium: In general the low frequency (white noise) limit of spectral density is lower than the high frequency limit (inverse Lorentz-behaviour) [6, 7, 11, 12] and in the time domain for $t > 0$ the autocorrelation function is negative [9]. This is a direct consequence that at equilibrium the linear current response is in opposite direction to an applied voltage pulse (c.f. [9]). For equal barrier height the spectral density and autocorrelation function (for $t > 0$) are constant (c.f. [12]). In both figures the low frequency limit decreases for higher barriers, because in

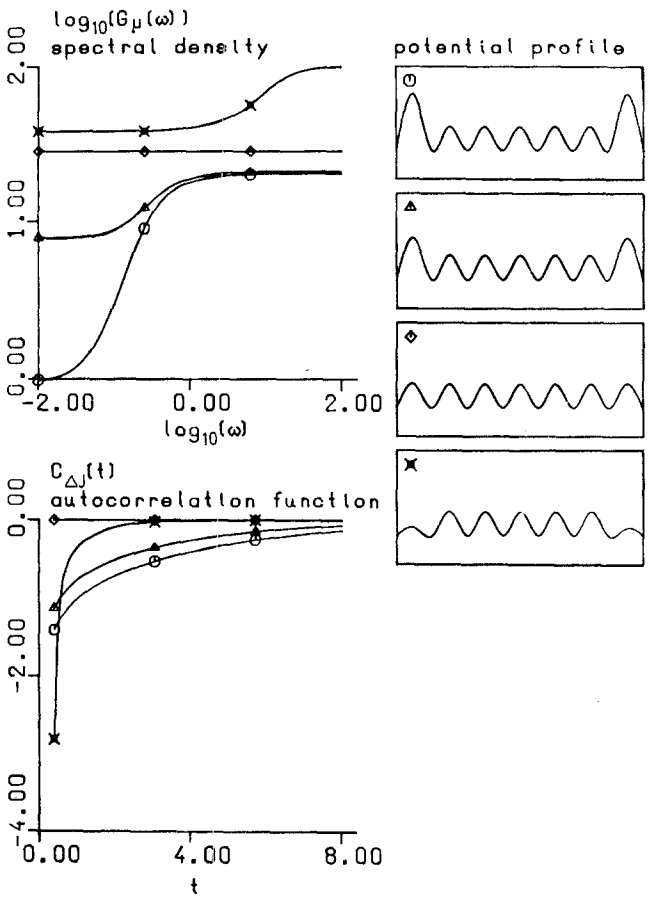

Fig. 2. Equilibrium current fluctuations in pores: variation of the height of decentral barriers. $n = 6$, $N_0 = N_{n+1} = 1$, $k_i' = k_i'' = 1$ for $i = 0,1,\ldots,n+1$ with the exceptions $k_0' = k_1'' = k_6' = k_7'' = \circ$ 0.01; $\triangle$ 0.1; $\Diamond$ 1; $\bowtie$ 10. All γ_i are chosen to be equal

these cases the steady state conductance, which according to the Nyquist theorem (2.21) is given by $G_{\Delta J}(\omega = 0)$, is smaller.

b) Non-Equilibrium: Relaxation Current After a Voltage Jump, Admittance, and Current Fluctuations

Figures 3–7 show the results of a number of numerical calculations for pores mainly under non-equilibrium conditions. The presentation is similar as in the preceeding figures. On the right-hand side the four potential profiles are drawn qualitatively in a suitable logarithmic presentation. The first potential profile (indicated by ○) denotes the equilibrium situation. The corresponding values of the equilibrium rate constants $\bar{k}_i'$, $\bar{k}_i''$ are given in the legends to the figures. In the other three cases the profile is changed by an applied voltage u. The voltage

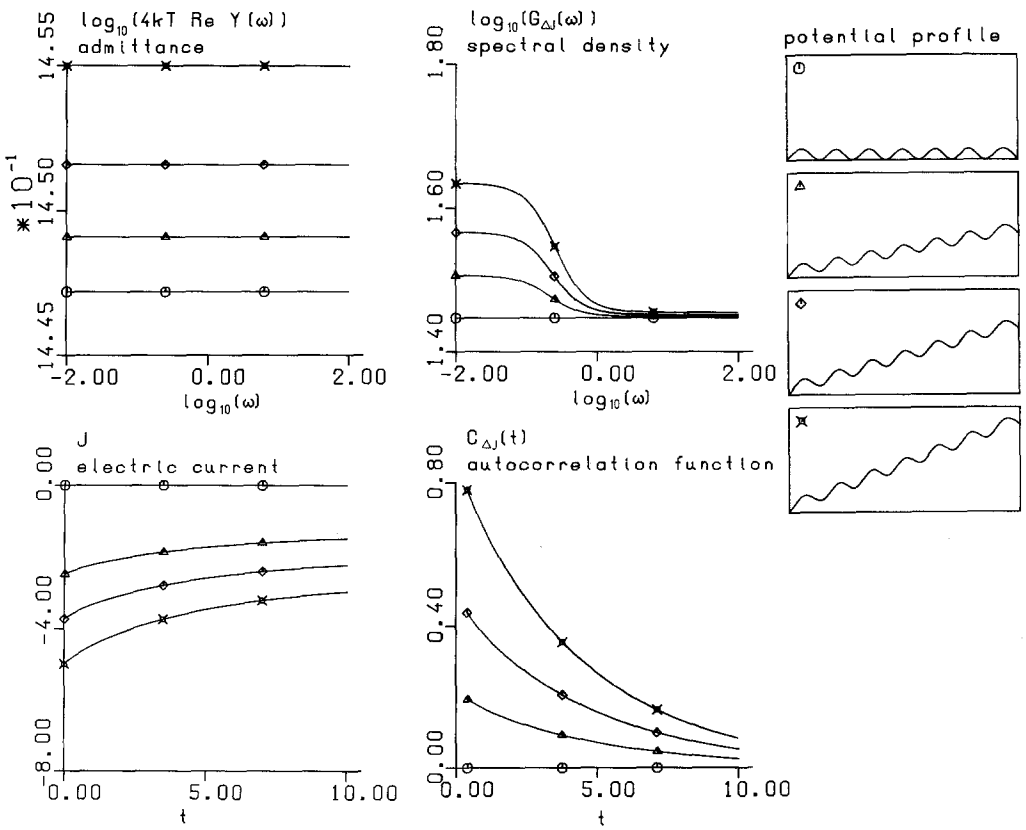

Fig. 3. Non-equilibrium: Relaxation current after a voltage, admittance and current fluctuations. Regular barrier structure. $n = 6$, $N_0 = N_{n+1} = 1$; all γ_i equal; $k_i' = k_i'' = 1$ for all $i = 0, 1, 2, \ldots, n + 1$. Voltage dependence of the rate constants: $k_i' = k_i' e^{-\frac{u/2}{n+1}}$, $k_i'' = k_i'' e^{+\frac{u/2}{n+1}}$. Applied (reduced) voltages u: $u = 0$, $u = 4/3$, $u = 2$, $u = 8/3$

dependence of the rate constants is given by (2.13). Spectral density and autocorrelation function are drawn in the same way as in the first two figures.

Furthermore, with the same choice of parameters, on the the left-hand side is drawn the real part of the admittance times $4\,kT$ as a function of frequency in the same arbitrary units as the spectral density. Thus both quantities can be compared. Note that the scales are different in Figs. 3 and 7. Finally the electric current after a voltage jump from the equilibrium situation indicated by ○ to one of the non-equilibrium situations △, ◊, ¤ is calculated and drawn on the bottom of the left-hand sides. Figure 3 shows the results for pores with regular energy profiles. The real part of the admittance is frequency-independent also at nonequilibrium states, while the spectral density of fluctuations for low frequencies increases with increasing u. This difference (for low frequencies) between $4\,kT\,Re\,Y(\omega)$ and $G(\omega)$ is called excess noise [9] of usual Lorentzian type.

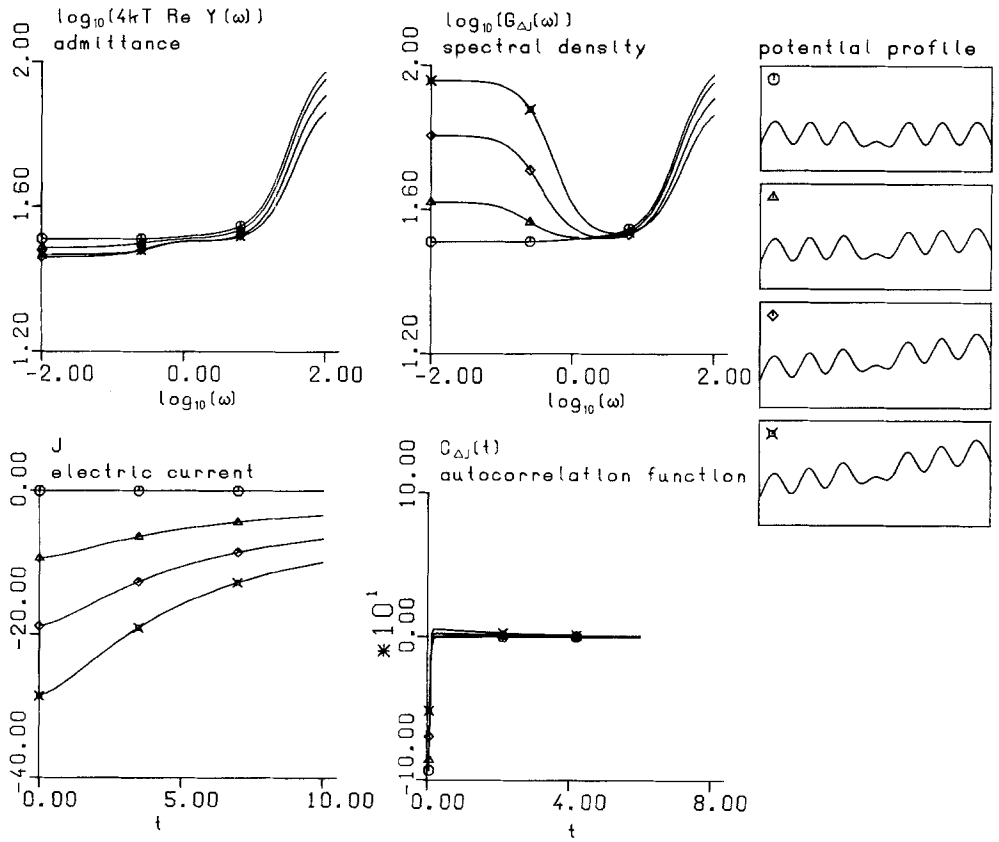

Fig. 4. Non-equilibrium: the effect of a low central barrier. $n = 6$, $N_0 = N_{n+1} = 1$; all γ_i equal; $k_i' = k_i'' = 1$ with the exceptions $k_3' = k_4' = 20$. Applied (reduced) voltages u: $u = 0$, $u = 2$, $u = 4$, $u = 6$

In the second example in Fig. 4 the influence of a low barrier within the pore is investigated, favouring the stay of ions in the central part of the pores. For low frequencies the comparison of $Re\, Y(\omega)$ and $G_{\Delta J}(\omega)$ again demonstrates the occurrence of typical Lorentzian excess noise. But on the contrary to the results for a regular barrier structure the spectral density at nonequilibrium has a strong minimum. The interpretation is as follows: The fluctuations come from a superposition of the global transport through the pore, being responsible for the excess fluctuations, and the transport fluctuations generated by the ionic jumps (in both directions) in the centre of the pores. The latter contribution to noise is similar to the transport noise generated by the movement of hydrophobic ions in a similar potential profile [11]. Furthermore, the increase of the frequency of ionic jumps by the lowered central barrier increases the white noise high frequency limit compared with the case of a regular barrier structure. In the time domain, comparison of the macroscopic relaxation current with the autocorrelation function of the current fluctuations yields a completely different behaviour in different time scales, though in principle the behaviour of both quantities is determined by the same time constants. The relaxations determined

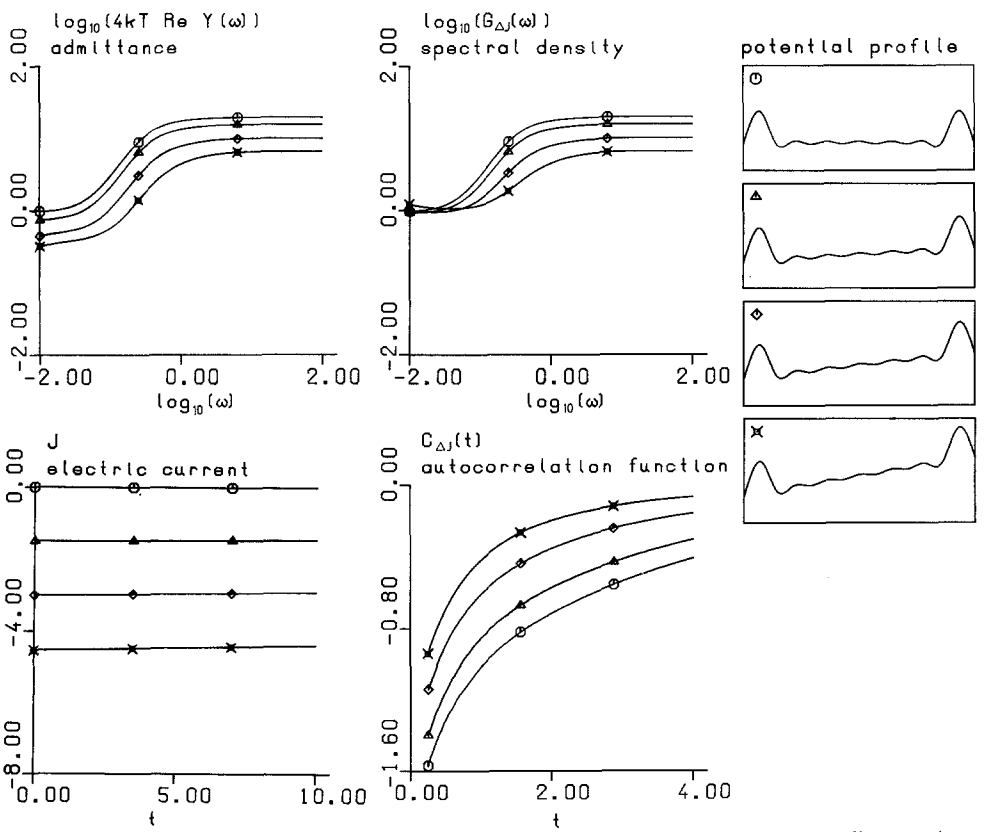

Fig. 5. Non-equilibrium: the effect of high decentral barriers. $n = 6$, $N_0 = N_{n+1} = 1$; all γ_i equal; $k_i' = k_i'' = 1$ with the exceptions $k_0' = k_1'' = k_6' = k_7'' = 0.02$. Applied voltages u: $u = 0$, $u = 2$, $u = 4$, $u = 6$

by these time constants occur with different amplitudes. This fact is demonstrated still more drastically in Fig. 5, where the relaxation current disappears completely, while the autocorrelation function shows a strong dependence on time.

In Fig. 5 the influence of high barriers regulating the influx into and efflux out of the pores is investigated. In this case the excess noise, i.e., the difference between $Y(\omega)$ and $G_{\Delta J}(\omega)$ for low frequencies, is less remarkable. The course of the spectral density is dominated by the ionic jumps within the pores and hence similar to the high frequency part in the example in Fig. 4. For increasing voltage u the high frequency limit decreases: a behaviour, which has been observed also in the current fluctuations generated by carrier transport [14]. It is a consequence of the fact that with increasing voltage and current the total rate of ionic jumps (in both directions), which determines the high frequency limits of $Re\, Y(\omega)$ and $G_{\Delta J}(\omega)$ [c.f. (2.20) and (2.26)], decreases because jumps in opposite direction to the applied field are suppressed.

A high central barrier within the pores has according to Fig. 6 a different influence on the properties of the system. In this case $4\,kT\, Re\, Y(\omega)$ and $G_{\Delta J}(\omega)$

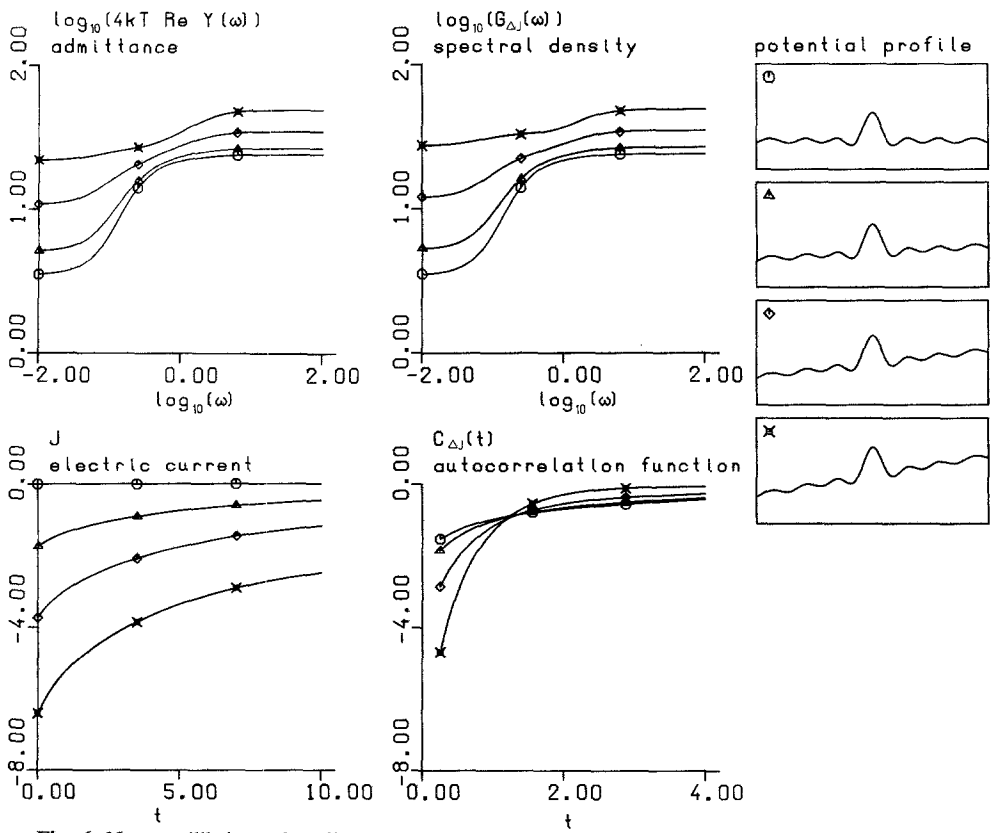

Fig. 6. Non-equilibrium: the effect of a high central barrier. $n = 6$, $N_0 = N_{n+1} = 1$; all γ_i equal; $k_i' = k_8'' = 1$ with the exceptions $k_3' = k_4'' = 0.01$. Applied voltages u: $u = 0$, $u = 2$, $u = 3$, $u = 6$

show a very similar behaviour in the whole frequency region. In both quantities occur two dispersive regions belonging to the two times of a) global ionic transport through the whole pore and b) transport in the right or left sides of the pores, which is dominated by 'reflection' at the high internal barrier.

Probably the reflections at the internal barrier are the reason for the fact that the high frequency limits are higher than the low frequency limits, because the number of ionic jumps is increased [and hence according to (2.20) and (2.26) the high frequency limits], without increasing the net flux through the pores.

Nevertheless, also in this example a general rule is confirmed, which we have recently proposed [8]: with increasing voltage the difference of current noise between the high and low frequency limits decreases. In case it is already negative, its absolute value increases.

Finally, for demonstration of the applicability of the numerical programme for more complex systems we have presented in Fig. 7 calculations for a barrier structure with 31 barriers and 30 binding sites and with a variable voltage

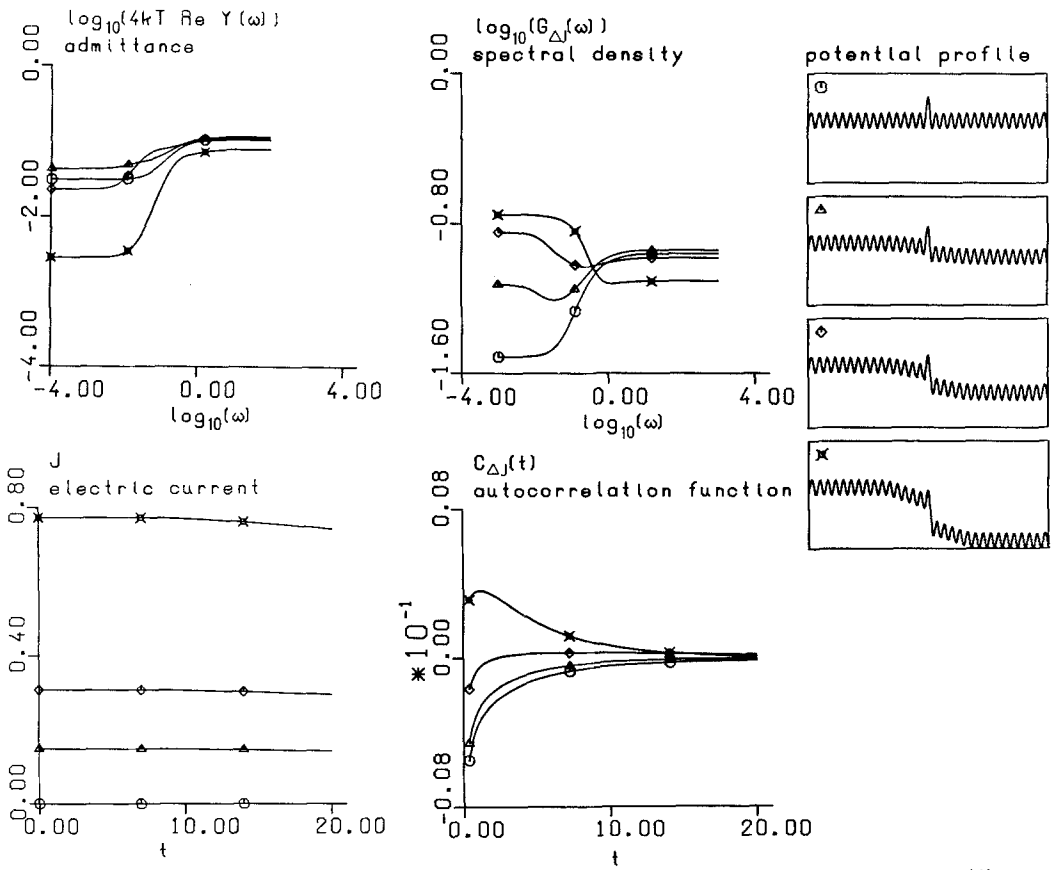

Fig. 7. Non-equilibrium: An example for a more complex structure. $n = 30$, $N_0 = N_{n+1} = 1$; $k_i' = k_i'' = 1$ with the exceptions $k_{15}' = k_{16}'' = 0.01$. $\gamma_i = 0$ for $i = 1, 2, \ldots, 10$; 0.05 for $i = 11, 12, \ldots, 15$; 0.5 for $i = 16$; 0.05 for $i = 17, 18, \ldots, 21$; 0 for $i = 22, 23, \ldots, 31$. Applied voltages u: $u = 0$, $u = 4$, $u = 8$, $u = 16$

dependence of the rate constants (see the legend to Fig. 7), causing a variable deformation of the potential for increasing voltage.

With increasing voltage the low frequency behaviour changes from an inverse Lorentzian structure to usual Lorentzian excess noise. In a special region (of voltage) $G_{\Delta I}(\omega)$ has a minimum. Comparison of the spectral density with the macroscopic admittance shows a strong difference for low frequencies due to the excess noise. The strong difference in the time behaviour of the macroscopic quantity 'current' (nearly constant) and the microscopic quantitiy 'autocorrelation function' is obvious.

Naturally, model calculations of this kind with high barrier numbers may be used for investigation of the influence of different transport regions in more complex systems. E.g., in Fig. 7 the central barrier may be regarded to represent the membrane. Then the neighbouring barriers and sites (in our example weakly voltage dependent) are the region, where the absorption and desorption processes between solution and membrane occur, and the region with negligible voltage dependence takes into account the influence of ionic diffusion in the aqueous solutions.

4. Conclusion

The presented numerical results may be useful to demonstrate the great complexity of the behaviour of transport systems as a function of their internal (fine) structure. These results may serve as a warning against the overinterpretation of and too specific conclusion from experimental results concerning problems as the barrier structure inside the pores. We have great doubts on such speculations.

On the other hand the great variety of the fluctuation properties (e.g., expressed in the results for the spectral density) demonstrates the strong influence of the internal fine structure of transport systems on the strength of the fluctuations (in different frequency regimes). During the evolution nature might have used these possibilities for an optimization of the transport systems, e.g., the minimization of noise. In this paper has been discussed a very simple transport model of pores without any interactions. In case interactions are included e.g., in the single-file model of narrow pores, the variety and complexity of the dependences of transport properties on internal parameters increases [6]. E.g., it seems likely that by the single-file mechanism the current fluctuations can drastically be reduced [13].

We believe that subject of future research on ion transport through biological membranes should be the problem of optimization according to their specific biological function. Possibly under this formulation of questions better established statements about the structure of the systems can be made.

References

1. Läuger P (1979) Transport of noninteracting ions through channels. In: Stevens CF, Tsien RW (eds) Membrane transport processes, vol. 3. Raven Press, New York, pp 17–27
2. Frehland E, Läuger P (1974) Ion transport through pores: transient phenomena. J Theor Biol 47: 189–207
3. Neher E, Sandblom J, Eisenmann G (1978) Ionic selectivity, saturation and block in gramicidin A channels. II. Saturation behaviour of single channel conductances and evidence for the existance of multiple binding sites in the channel. J Membr Biol 40: 97–116
4. Lewis CA, Stevens CF (1979) Mechanism of ion permeation through channels in a postsynaptic membrane. In: Stevens CF, Tsien RW (eds) Membrane transport processes, vol. 3. Raven Press, New York, pp 133–151
5. Begenisich T, Cahalan M (1979) Non independence and selectivity in sodium channels. In: Stevens CF, Tsien RW (eds) Membrane transport processes, vol. 3. Raven Press, New York, pp 113–122
6. Frehland E, Stephan W (1979) Theory of single-file noise. Biochim Biophys Acta 553: 326–341
7. Frehland E (1978) Current noise around steady states in discrete transport systems. Biophys Chem 8: 255–265
8. Frehland E (1979) Theory of transport noise in membrane channels with open-closed kinetics. Biophys Struct Mech 5: 91–106
9. Frehland E (1980) Current fluctuations in discrete transport systems far from equilibrium – Breakdown of the fluctuation dissipation theorem. Biophys Chem 12: 63–71
10. Zwolinsky BJ, Eyring H, Reese CE (1949) Diffusion and membrane permeability. J Phys Chem 53: 1426–1453
11. Kolb H-A, Läuger P (1977) Electrical noise from lipid bilayer membranes in the presence of hydrophobic ions. J Membr Biol 37: 321–345
12. Läuger P (1978) Transport noise in membranes. Current and voltage fluctuations at equilibrium. Biochim Biophys Acta 507: 337–349
13. Frehland E (1980) (to be published)
14. Kolb H-A, Frehland E (1980) Noise-current generated by carrier-mediated ion transport at non-equilibrium. Biophys Chem 12: 21–34

Received March 10, 1980/Accepted June 18, 1980